

BALANCING STABILITY AND PLASTICITY IN CONTINUAL LEARNING: THE READOUT-DECOMPOSITION OF ACTIVATION CHANGE (RDAC) FRAMEWORK

Daniel Anthes*, Sushrut Thorat*, Peter König, & Tim C. Kietzmann

Institute of Cognitive Science

Osnabrück University

Osnabrück, 49090, Germany

{danthes, sthorat, pkonig, tkietzma}@uos.de

ABSTRACT

Continual learning (CL) algorithms strive to acquire new knowledge while preserving prior information. However, this stability-plasticity trade-off remains a central challenge. This paper introduces a framework that dissects this trade-off, offering valuable insights into CL algorithms. The Readout-Decomposition of Activation Change (RDAC) framework first addresses the stability-plasticity dilemma and its relation to catastrophic forgetting. It relates learning-induced activation changes in the range of prior readouts to the degree of stability, and changes in the null space to the degree of plasticity. In deep non-linear networks tackling split-CIFAR-110 tasks, the framework clarifies the stability-plasticity trade-offs of the popular regularization algorithms Synaptic intelligence (SI), Elastic-weight consolidation (EWC), and learning without Forgetting (LwF), and replay based algorithms Gradient episodic memory (GEM), and data replay. GEM and data replay preserved both stability and plasticity, while SI, EWC, and LwF traded off plasticity for stability. The inability of the regularization algorithms to maintain plasticity was linked to them restricting the change of activations in the null space of the prior readout. Additionally, for one-hidden-layer linear neural networks, we derived a gradient decomposition algorithm to restrict activation change only in the range of the prior readouts, to maintain high stability while not further sacrificing plasticity. Results demonstrate that the algorithm maintained stability without significant plasticity loss. The RDAC framework not only informs the behavior of existing CL algorithms but also paves the way for novel CL approaches. Finally, it sheds light on the connection between learning-induced activation/representation changes and the stability-plasticity dilemma, also offering insights into representational drift in biological systems.

1 INTRODUCTION

Continual learning (CL) is a fundamental challenge in the field of neural networks, aiming to equip these learning systems with the ability to acquire new knowledge while not forgetting previously learned information, which is termed the stability-plasticity dilemma (Carpenter & Grossberg, 1987; Mermillod et al., 2013). In the common setting of gradient-based learning in neural networks, performance on prior tasks reduces as new tasks are learned i.e. stability is traded off for plasticity. This phenomenon is termed catastrophic forgetting (McCloskey & Cohen, 1989; French, 1999).

Much of the catastrophic forgetting has been linked to learning-induced changes that occur in the later layers of neural networks (Ramasesh et al., 2020; Kalb & Beyerer, 2022). Moreover, recent work revealed that, during task-incremental learning (van de Ven et al., 2022), a large portion of the loss in task performance is not about the information relevant to the previous tasks being forgotten.

*indicates equal contribution.

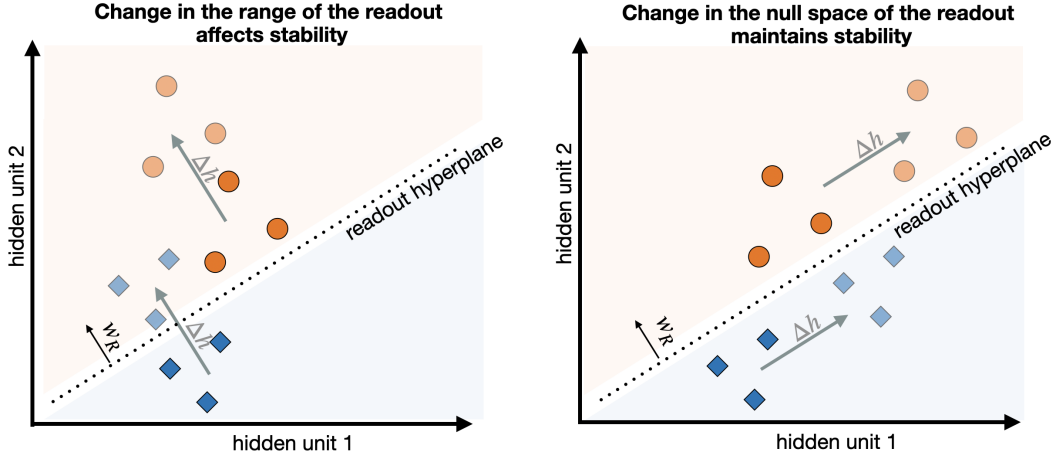


Figure 1: Conceptualization of the readout-decomposition of activity change. The readout for a task reads from a subspace of the pre-readout activation space. In the case of a two dimensional activation space, and a binary readout, the hyperplane defines a line through the 2D space. (Left) Any gradient affecting this space in a way that changes activation patterns perpendicular to the hyperplane (the range of the readout) affects the mapping between hidden and readout activations, and is detrimental to stability. (Right) Any gradient affecting this space in a way that changes activation patterns parallel to the hyperplane (the null space of the readout) does not affect the mapping between hidden and readout activations. However, this change is useful for learning new tasks i.e. being plastic, while not disrupting stability.

Instead due to learning the activations change, and the prior readout hyperplanes no longer align with the discriminative directions in the activations (Davari & Belilovsky, 2021; Anthes et al., 2023). Seeking to generalize these results, we introduce a framework to study what aspects of the learning-induced activation changes, from the perspective of the prior readouts, are related to the performance on prior tasks and to the performance on future tasks.

We present the Readout-Decomposition of Activation Change (RDAC) framework. The central principle is as follows: Learning-induced activation changes within the range of prior readouts (the subspace of pre-readout activation space spanned by the readout vectors) can lead to the task-relevant activations being misaligned with the readouts, thereby reducing the degree of stability. If thereby changes in the range are minimal, changes in the null space are critical as they reflect the network learning new tasks. If the changes to the null space are also restricted, the network won't be able to learn new tasks, thereby reducing the degree of plasticity. This principle is depicted in Figure 1.

The RDAC framework serves as a diagnostic tool to assess the stability-plasticity trade-offs of CL algorithms. Moving beyond performance-based comparisons, we can compare the learning-induced activation changes in the range and null space of the prior readouts to reveal the causes of the observed performance trade-offs. In this work, we assessed the stability-plasticity trade-offs of popular CL algorithms - three regularization algorithms: Synaptic intelligence (SI; Zenke et al. (2017)), Elastic-weight consolidation (EWC; Kirkpatrick et al. (2017)), and Learning without forgetting (LwF; Li & Hoiem (2017)), and two replay algorithms: Gradient episodic memory (GEM; Lopez-Paz & Ranzato (2017)), and data replay (Rebuffi et al., 2017). Our results revealed that during learning the split-CIFAR-110 tasks, SI, EWC, and LwF restricted the activation changes in both the range and null space of prior readouts, thereby trading off plasticity for the sake of stability. Meanwhile, GEM and data replay did not restrict activation change in the null space, maintaining high plasticity. Intriguingly, the activation change in the range was also not restricted completely, while the stability was still observed to be high in the task performance. We reasoned that this is due to the non-linear, many-to-one mapping allowed by the loss functions used by GEM and data replay. In sum, we demonstrate the usefulness of RDAC in furthering our understanding of how continual learning algorithms function at the level of the activations and the weights in the networks.

The RDAC framework can also be used to develop new continual learning algorithms. We demonstrate how we can translate the core principle of RDAC into a gradient decomposition algorithm in simple one-hidden-layer linear networks. We tested that algorithm in a network learning the split-MNIST tasks. We found that the stability-plasticity trade-offs are linked to the activation changes in the range and null space of the prior readout, and we can exert full control over them with two parameters. Additionally, in the best setting, the algorithm maintains stability and plasticity close to the upper bounds set by the task. In sum, we demonstrate the usefulness of RDAC taking the first steps in building new CL algorithms.

The RDAC framework primarily helps in assessing the stability-plasticity trade-offs in existing CL algorithms. Additionally, the principles of the framework pave the way for the development of novel CL approaches. Furthermore, the relationship between learning-induced activation/representation changes and the stability-plasticity dilemma offers insights into representational drift in biological systems. By shedding light on these critical aspects of CL, this paper contributes to the ongoing efforts to characterize the complexities of continual learning in order to solve it.

2 RELATED WORK

In the landscape of research addressing the challenges of continual learning (CL), several noteworthy contributions have emerged that offer valuable insights into the stability-plasticity trade-off and related concepts (Parisi et al., 2019; De Lange et al., 2021; Mundt et al., 2023; Wang et al., 2023; Kim & Han, 2023). Most of these approaches compare the different CL algorithms in terms of their performance on previously-learned tasks as a function of learning new tasks and ablations on the various components of those algorithms. We seek to characterize the stability-plasticity trade-offs of the algorithms in terms of the changes in weights and prior tasks’ activations. In addition to investigating how well algorithms solve the catastrophic forgetting problem, we place special emphasis on the algorithms’ continued ability to learn new tasks i.e. their plasticity.

Recently, many groups have sought to understand the influence of learning-induced activation changes on stability and plasticity (Wang et al., 2021; Kong et al., 2022; Zhao et al., 2023; Yang et al., 2023). All these approaches analyze the gradient updates in the range of the space spanned by the activations for previous tasks, for each layer of the network. However, it is unclear whether the range of the readouts, which determines the outputs of the network, is equivalent to the range of the activations for the previous tasks. The range of the activations is most probably larger than the range of the readouts, and the pre-readout activation space is usually very high-dimensional compared to the readout. Also, prior work has shown that the activation space contains classification-orthogonal information (e.g. size and location of the object; Hong et al. (2016); Thorat et al. (2021)), which implies the activation space has more information than required by the readout. If the range of the activations is indeed larger, the space in which activations could change, while maintaining the previous tasks’ performance, would seem smaller. This would suggest a reduced capacity for learning future tasks. To circumvent this potential issue, in the RDAC framework, we provide a different view on the link between the activation change and the stability-plasticity trade-off, by directly focusing on the range of the readouts.

3 THE READOUT-DECOMPOSITION OF ACTIVATION CHANGE FRAMEWORK

In the RDAC framework, we link the performance-based stability-plasticity trade-offs of continual learning algorithms to how they constrain learning. First, we study how learning-based changes in prior task activations, in the range and null space of the prior readout, is linked to stability and plasticity. Second, in one-hidden-layer linear neural networks, we show how the activation changes are linked to the weight updates, and derive a gradient-decomposition-based algorithm to ensure maximal stability without further throttling plasticity.

3.1 READOUT-DECOMPOSITION OF ACTIVATION CHANGE TO DIAGNOSE THE STABILITY-PLASTICITY TRADE-OFF

In task-incremental continual learning, a network has to sequentially learn a set of n task mappings $\{\mathbf{x}^k \rightarrow \mathbf{o}^k\}_{k \leq n}$. The network’s weights are shared across tasks, except for the readouts,

$\{\mathbf{W}_{\mathbf{R}^k}\}_{k \leq n}$, which are task specific. For a given task $k < m$, consider the pre-readout activations \mathbf{h}^k such that $\mathbf{o}^k = \sigma(\mathbf{h}^k \mathbf{W}_{\mathbf{R}^k}^\top + \mathbf{b}_{\mathbf{R}^k}^\top)$, σ is a non-linear activation function and b is the readout bias. While learning on the new task m , we posit that the change in activations, $\Delta \mathbf{h}^k$, can be decomposed as $\Delta \mathbf{h}^k \mathbf{C} \mathbf{C}^\top + \Delta \mathbf{h}^k \mathbf{N} \mathbf{N}^\top$, where \mathbf{C} and \mathbf{N} are the range and null-space matrices of $\mathbf{W}_{\mathbf{R}^k}$, and $\mathbf{C} \mathbf{C}^\top$ and $\mathbf{N} \mathbf{N}^\top$ are the corresponding projection matrices. These two components can provide us insights into the stability-plasticity trade-offs of a given learning algorithm.

First, changes in the activations in the range of the readout ($\Delta \mathbf{h}^k \mathbf{C} \mathbf{C}^\top$) could disrupt stability as $\Delta \mathbf{h}^k \mathbf{C} \mathbf{C}^\top \mathbf{W}_{\mathbf{R}^k} = \Delta \mathbf{h}^k \mathbf{W}_{\mathbf{R}^k}$. Second, changes in the activations in the null space of the readout ($\Delta \mathbf{h}^k \mathbf{N} \mathbf{N}^\top$) would have no effect on stability, as $\Delta \mathbf{h}^k \mathbf{N} \mathbf{N}^\top \mathbf{W}_{\mathbf{R}^k} = \mathbf{0}$. Monitoring these components of the activation changes can provide us with valuable insights into the inner workings of continual learning algorithms, which is what we present in Section 4.

However, it is important to note that if the non-linearity σ performs a many-to-one mapping, it can effectively negate the influence of those “degenerate” activation changes on the output. Thus, certain learning algorithms could lead to a change of activations in the range of the readout, even though their performance on previous tasks, i.e. stability, would be unchanged.

Under this framework, assuming no knowledge about the non-linearities involved, a “conservative” continual learning algorithm would clamp the pre-readout activations for the previously learned tasks in the range of the corresponding readouts to ensure stability. The activations would not be clamped in the null space of those readouts to ensure plasticity.

3.2 DERIVING A GRADIENT DECOMPOSITION ALGORITHM TO CONTROL THE STABILITY-PLASTICITY TRADE-OFF

The input-output mapping of a one-hidden-layer linear network, with no bias terms, can be written as $\mathbf{o} = \mathbf{x} \mathbf{W}_{\mathbf{H}}^\top \mathbf{W}_{\mathbf{R}}^\top$, where $\mathbf{o}^{1 \times o}$ is the output with o neurons, $\mathbf{x}^{1 \times x}$ is the input with x features, $\mathbf{W}_{\mathbf{H}}^{h \times x}$ is the mapping from input to the hidden layer with h neurons, and $\mathbf{W}_{\mathbf{R}}^{o \times h}$ is the mapping from the hidden layer to the output. After training on task 1: $\mathbf{x}^1 \rightarrow \mathbf{o}^1$, we get the trained readout $\mathbf{W}_{\mathbf{R}^1}$. While training on task 2: $\mathbf{x}^2 \rightarrow \mathbf{o}^2$, we get the gradient $\Delta \mathbf{W}_{\mathbf{H}}$. In order to maintain stability, we want the learned task 1: $\mathbf{x}^1 \rightarrow \mathbf{o}^1$ mapping to stay preserved.

Given a projection matrix $\mathbf{A}^{h \times h}$ applied to the gradient, we want:

$$\mathbf{o}^1 = \mathbf{x}^1 (\mathbf{W}_{\mathbf{H}} + \mathbf{A} \Delta \mathbf{W}_{\mathbf{H}})^\top \mathbf{W}_{\mathbf{R}^1}^\top \implies \mathbf{x}^1 (\mathbf{A} \Delta \mathbf{W}_{\mathbf{H}})^\top \mathbf{W}_{\mathbf{R}^1}^\top = \mathbf{0} \implies \mathbf{W}_{\mathbf{R}^1} \mathbf{A} = \mathbf{0} \quad (1)$$

One solution is $\mathbf{A} = \mathbf{N} \mathbf{N}^\top$, where \mathbf{N} is the null space matrix of $\mathbf{W}_{\mathbf{R}^1}$. Projecting the gradient for the $\mathbf{W}_{\mathbf{H}}$ into the null space of $\mathbf{W}_{\mathbf{R}^1}$ will ensure stability. Meanwhile, the hidden layer activations \mathbf{h}^1 are free to change in the null space of $\mathbf{W}_{\mathbf{R}^1}$ which allows plasticity.

To allow full control over the stability-plasticity trade-off, we can consider $\mathbf{A} = \alpha \mathbf{C} \mathbf{C}^\top + \beta \mathbf{N} \mathbf{N}^\top$, where α (termed “range weight”) and β (termed “null space weight”) are scalars that weigh the projections into range and null space of $\mathbf{W}_{\mathbf{R}^1}$. $\mathbf{W}_{\mathbf{R}^1} \mathbf{A} = \mathbf{0}$ only if $\alpha = 0$, which ensures stability. Stability does not rely on β but plasticity does as, if β is reduced while $\alpha = 0$, the gradient becomes smaller and learning the new task becomes slower. In Section 5, we empirically test this relationship between α , β , and the stability-plasticity trade-off.

In learning multiple tasks sequentially, \mathbf{N} can be computed from the null space of the stacked readout matrices of the n previous tasks, $\mathbf{W}_{\mathbf{R}}^{t \times h}$, where $t = \sum_{k=1}^n n o_k$, and o_k are the number of classes in task k . With $\mathbf{A} = \mathbf{N} \mathbf{N}^\top$, none of the previously learned task mappings would be affected. It is interesting to note that if the tasks are not all fully orthogonal and rely on shared features, the range of the stacked readout matrices would grow sub-linearly with the addition of new output units.

The introduction of non-linearities and multiple hidden layers makes the procedure seen in Equation 1 non-trivially complex and beyond the purvey of this paper. We leave the search for approximate solutions that might guide a generic gradient-decomposition-based algorithm as a quest for the future. Although we do not present a continual learning algorithm for deep non-linear networks, we hope that the intuitions garnered through the derivation in this simple case pave the way.

4 CONTINUAL LEARNING IN DEEP NON-LINEAR NEURAL NETWORKS

Using the RDAC framework, we present an assessment of how a variety of continual learning algorithms allow changes in the activations and how those changes relate to the observed performance-based stability-plasticity trade-offs. First, we outline the network architecture and task setting. Then, we present the results comparing the different learning algorithms: three regularization methods - Synaptic Intelligence (SI; Zenke et al. (2017)), EWC, and Learning without Forgetting (LwF; Li & Hoiem (2017)) - and two replay-based methods - Gradient Episodic Memory (GEM; Lopez-Paz & Ranzato (2017)) and data replay¹(Rebuffi et al., 2017). In addition to them being popular, these algorithms were chosen due to the availability of their implementations through the Avalanche library (Carta et al., 2023).

4.1 NETWORK AND TASK

We considered a VGG-like neural network, similar to the one used in Zenke et al. (2017), which maps CIFAR images (Krizhevsky et al., 2009) to their classes (The exact architecture and optimization procedure is described in Appendix A.1.1). We considered the split-CIFAR-110 setting, where the network is first trained on CIFAR-10, and then sequentially trained on ten equal task splits from CIFAR-100 (we ran the analysis 3 times with randomly chosen assignments of classes to splits, and show the results averaged across those seeds). Images were subjected to augmentations. Separate readouts were trained for each of the tasks, with softmax activation and cross-entropy loss. After training on task 1 (CIFAR-10), we computed the projection matrices CC^\top and NN^\top , using singular value decomposition (SVD).

4.2 RESULTS

In terms of performance, how do the different learning algorithms manage the stability-plasticity trade-off? We considered the performance on task 1 (a measure of stability) and on task 11 (a measure of plasticity) after training on all 11 tasks. As seen in Figure 2A, as the regularization strength was increased, EWC, SI, and LwF traded off plasticity for stability. On the other hand, with increasing replay buffer size (and memory strength in the case of GEM), GEM and data replay managed to increase stability without trading off plasticity. We now assess these stability-plasticity trade-offs from the perspective of the RDAC framework.

First, the RDAC framework associates restricting the change in prior tasks’ activations in the null space of the prior readouts with a loss in plasticity. Were SI, EWC, and LwF unable to maintain plasticity, compared to GEM and data replay, because they imposed higher restrictions on the change in the activations for task 1 in the range of the task 1 readout? Yes, as seen in Figure 2B, increasing the regularization strength for SI, EWC, and LwF, substantially reduced the learning-induced changes in the task 1 activations in the null space of task 1 readout. Meanwhile, increasing the replay buffer size (and memory strength in the case of GEM), for GEM and data replay, did not lead to a similarly drastic reduction in the activation changes in the null space. Restricting change in range is desirable, but these regularization algorithms restricted change in null space too, which was detrimental to plasticity. In contrast, GEM and data replay maintained higher activation changes in the null space, corresponding to higher observed plasticity.

Interestingly, with increasing replay buffer size and memory strength in GEM, the activation change in the null space increased. This can be explained by understanding how GEM computes its gradient projection. GEM solves a constrained optimization problem to project the current gradient such that its dot product with gradients estimated for the previous tasks (estimated with the replay buffer) is positive. The replay buffer size determines how well the mappings for the old task are preserved. The insistence on a positive dot product ensures that the gradient update is aligned with the gradient directions expected by the previous tasks, which maintains stability. Additionally, the gradient is further biased towards the gradients for the previous tasks with a “memory strength” parameter γ . As γ increases, the gradients from all the previous tasks get weighted up in the gradient used by

¹In data replay and LwF, contrary to the usual setting, we fixed readouts after training on a task and allowed the rest of the network to train further. This was done because in all the other methods, the prior readouts are frozen.

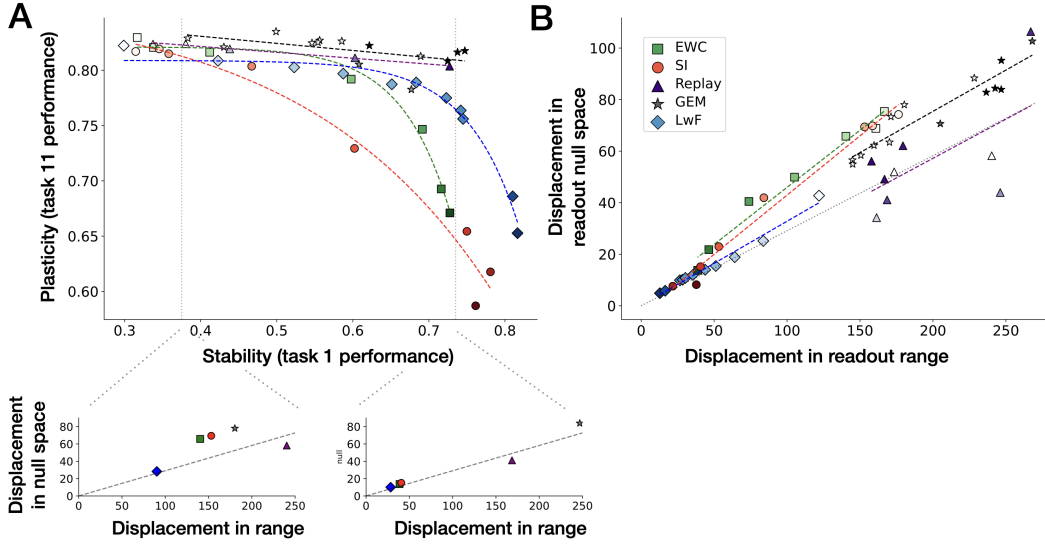


Figure 2: Continual learning in deep non-linear neural networks learning to classify CIFAR images. (A) With increasing regularization strength, replay buffer size, and memory strength (indicated with darkening hues), the stability of all the algorithms increases. However, the replay algorithms, GEM and data replay maintain high plasticity, whereas the regularization algorithms do not do so. (B) In the pre-readout activation space, the activation change is quantified as the difference between task 1 activations after training on task 1 and after training on all 11 tasks (displacement). With increasing regularization strength, the regularization algorithms reduce the activation change in both the range and null space of task 1 readout, which corresponds to the observed maintenance of stability and loss of plasticity. With increasing replay buffer size (and memory strength in the case of GEM), the replay algorithms maintain high activation change in both the range and null space of the task 1 readout, which ensures plasticity. The use of non-linear, many-to-one mapping loss functions by these algorithms allow for changes in the range that are not detrimental to stability. These results illustrate the utility of the RDAC framework as a diagnostic tool to understand the stability-plasticity trade-offs of continual learning algorithms. The diagonal dotted line in panel B and the two insets indicate the expected ratio of displacement in null space and range of a readout if activations were to move uniformly in all dimensions of the pre-readout layer.

GEM. From the standpoint of readout 1 this would mean more projections into its null space which would result in an increased change of its activations in its null space after training on multiple tasks.

Second, the RDAC framework associates activation changes in the range of the readout with a loss in stability. With increasing regularization strength, SI, EWC, and LwF, indeed substantially reduced the activations changes in the range of the readout, corresponding to an increase in stability. In the case of data replay, although increasing the replay buffer size led to an increase in stability, the reduction in the activations changes in the range of the readout was not substantial. Relatedly, in the case of GEM, with increasing replay buffer size and memory strength, the activation changes in the range of the readout increased.

How do we reconcile these observations with the RDAC framework? The critical element is the nature of the gradient constraints imposed by GEM and data replay. Both GEM and data replay compute the gradients for the prior tasks to optimize the mapping between images and the “true” labels, as opposed to the probability distribution over labels previously learned by the network. The mapping between probability distributions and the 1-hot probability distribution given by the true label, under cross-entropy loss, is degenerate. As expressed in the RDAC framework, activation changes in the range can be negated by such a non-linearity. Thus, GEM and data replay are allowed gradient projections that lead to changes in activations in the range of the prior readouts. This ability is specific to replay-based methods as they have access to the expected mappings for the prior tasks which help them in knowing what parts of the range of the prior readouts can be changed without affecting those prior mappings.

Additionally, in the case of GEM, increasing the memory strength increases the contributions of the gradients of the prior tasks to the estimated gradient. Gradients for the prior tasks are meant to reduce the loss for those tasks, which implies they would project into the corresponding ranges of the prior readouts. This explains the increased activation change in the range of the prior readout. The function of these changes in the range of the readout potentially is to supplement performance on the previous tasks, a phenomenon termed “backward transfer” (Lopez-Paz & Ranzato, 2017).

In sum, our results show that the principles laid out in the RDAC framework relating readout-decomposed activation changes to the stability-plasticity trade-offs provide useful insights into the inner workings of continual learning algorithms for deep, non-linear neural networks.

5 CONTINUAL LEARNING IN ONE HIDDEN-LAYER LINEAR NEURAL NETWORKS

Using the RDAC framework, we present an assessment of the stability-plasticity trade-offs of the gradient decomposition algorithm derived in Section 3.2. First, we outline the network architecture and task setting. Second, we present the results assessing our control over the stability-plasticity trade-off given our algorithm. Third, to understand the complexity of the network and task setting, we assess the stability-plasticity trade-offs of EWC. We chose EWC due to its popularity, the relative ease of its implementation outside the Avalanche library, and because it has only one regularization parameter.

5.1 NETWORK AND TASK

We considered a neural network with one hidden layer with 11 neurons with no bias terms, which maps MNIST images (LeCun et al., 1998) to their classes (The exact architecture and optimization procedure is described in Appendix A.1.2). We considered the split-MNIST setting where the first task is to classify the first five digits (0-4), and the second task is to classify the last five digits (5-9). Images were subjected to augmentations. Separate readouts were trained for the two tasks, with softmax activation and cross-entropy loss. After training on task 1, we computed the projection matrices $\mathbf{C}\mathbf{C}^\top$ and $\mathbf{N}\mathbf{N}^\top$, using SVD.

5.2 RESULTS

First, we assessed if the gradient decomposition algorithm managed to maintain stability without trading off plasticity, and whether varying the range and null space weights (α and β) led to the control over the stability-plasticity trade-off outlined in the RDAC framework. As seen in Figure 3A, when $\alpha = 0$ and $\beta = 1$, the performance on both task 1 (stability) and on task 2 (plasticity) was high. We also observed no task 1 activation change in the readout 1 range, but observed substantial change in the null space which corresponds to the network learning task 2 (Figure 3B). Increasing α to 1 increased the activation change in the readout range, thereby reducing the stability. On the other hand, lowering β to 0 decreased the activation change in the readout null space, thereby reducing the plasticity. These simulations both show the efficacy of the gradient decomposition algorithm and confirm the control over the stability-plasticity trade-off outlined in the RDAC framework.

Next, to assess the complexity of the split-MNIST task in a one-hidden-layer linear network, we assessed the stability-plasticity trade-offs of EWC. If it is trivial to jointly maintain stability and plasticity, we reasoned that EWC can fare well on this task as compared to the task in the previous section. As seen in Figure 3A, increasing the regularization strength of EWC increased the stability at the expense of plasticity. Analyzing the activation change in the readout range and null space revealed that EWC ended up restricting change not only in the range (which is useful for stability) but also in the null space which was detrimental to plasticity (Figure 3B). This indicates that the network and task settings in use constitute a non-trivial continual learning problem.

These results confirm that the principles of the RDAC framework can be fruitfully put into practice.

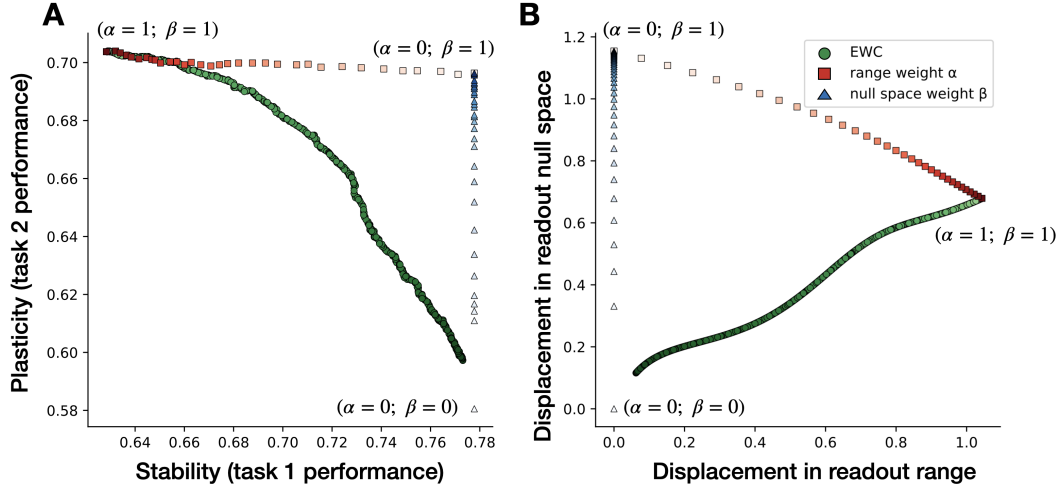


Figure 3: Continual learning in one hidden-layer linear neural networks learning to classify MNIST digits. (A) The gradient decomposition algorithm can maintain both stability and plasticity when the gradients are projected into the null space of the previous readout ($\alpha = 0$, $\beta = 1$). Allowing the gradients to be projected into the range of the readouts ($\alpha > 0$) is detrimental to stability, whereas restricting the gradients from being projected into the null space of the readouts ($\beta < 1$) is detrimental to plasticity. Additionally, Elastic weight consolidation (EWC) trades off plasticity for stability, indicating that this problem is non-trivial from a continual learning standpoint. Darker hues correspond to higher values of α , β , and the EWC regularization strength λ . (B) In the hidden-layer activation space, the gradient decomposition algorithm effectively restricts changes in the activations for task 1 to the null space of the task 1 readout. Restricting the change in the null space is detrimental to plasticity, as seen in the case of EWC and when we set $\beta < 1$. These results illustrate the utility of the RDAC framework in informing the construction of new continual learning algorithms.

6 DISCUSSION

In this study, we introduced the Readout-Decomposition of Activation Change (RDAC) framework which provides a unique perspective on the stability-plasticity dilemma in continual learning, by viewing the continual learning problem from the standpoint of the readout layer. The core insight is as follows. Readouts span a subspace (the range) in activation space. Restricting learning from making changes to the projections of the activations of prior tasks to that subspace is sufficient to ensure stability. Further restricting any change to the activations in the subspace other than that spanned by the readout (the null space) is detrimental to plasticity. We analyzed popular continual learning algorithms and provided insights into the trade-offs these algorithms make in terms of stability and plasticity, and how they relate to changes in the activations for prior tasks from the perspective of the prior readouts. Additionally, given the insights from the framework, for one-hidden-layer linear networks, we derived a gradient decomposition algorithm that restricts learning-induced activation changes to only the null space of prior readouts to maintain plasticity while ensuring stability.

The regularization-based algorithms, SI, EWC, and LwF, traded off plasticity substantially for stability. In contrast, the gradient decomposition algorithm and the replay-based algorithms managed to maintain high plasticity and stability. We suspect that reliance on Sherringtonian notions of information processing (Barack & Krakauer, 2021), in the case of SI and EWC, is the cause of this discrepancy. Usually the hyperplanes are not axis-aligned (Morcos et al., 2018), as schematized in Figure 1). If the importance scores are computed at the level of the individual weights (corresponding to the two hidden neurons) in the setting in Figure 1, both the weights/axes would have high importance scores. The regularization algorithms would weigh down learning in both the weights. However, a regularization algorithm relying on the principal dimensions of the learning in weight space (a Hopfieldian approach) could identify the subspace in which both the weights are allowed to

change, thereby increasing the capacity to learn new tasks while preserving stability. The theoretical analysis and empirical testing of this idea are interesting avenues for future work.

The replay-based algorithms, GEM and data replay, maintained higher plasticity than the regularization-based algorithms, given the same amount of stability. Crucially, we observed that the activation changes in the range of the readout were higher than expected and proposed that it could be traced back to a degenerate solution space imposed by the non-linearity in the loss function. The regularization-based algorithm, LwF, also enjoyed such degeneracy provided by the loss function. However, there are two points of divergence between LwF and the replay-based algorithms. One, the estimates of the gradients for prior tasks were computed using the data seen during ongoing learning, which were potentially bad approximations. Two, the loss was computed using the probability distribution over prior readouts, termed “pseudo-labels”, which potentially provided a lower degree of degeneracy than a 1-hot true-label distribution provided. These two aspects might have contributed to LwF being unable to change activations in the range as much as GEM and data replay did. Moving forward, extensions of the RDAC framework analytically to non-linear settings would be crucial to shed light on the learning dynamics in such algorithms.

An intriguing facet of our framework lies in its demonstration that activation changes within the null space of the readout are essential for learning. Consider the following situation: an observer unaware of the continual learning algorithm observes the network activations for a fixed set of stimuli over learning. The activations would keep changing across time which could make the observer wonder how the network reads out of such a dynamic code. Moreover, in the case where the loss functions used by the algorithm are non-linear, the resultant degeneracy might make any readout trained by the observer at a time point harder to generalize to other time points. These signatures of activation change and the optimal-readout changing over time have been observed in mammalian brains, and the activation change is termed “representational drift” (Driscoll et al., 2017). Recently it has been suggested that the reason drift exists is because animals are engaged in learning (Aitken et al., 2022; Masset et al., 2022; Driscoll et al., 2022; Micou & O’Leary, 2023). This suggestion dovetails with the RDAC framework under which, drift, especially in the null space of the readout, is indispensable to continual learning.

The RDAC framework is designed with a focus on task-incremental learning, where new readouts are trained for each task encountered during the continual learning process, and the prior readouts are frozen. There exist other continual learning scenarios van de Ven et al. (2022), some in which the readout layer can always be learnable (Rebuffi et al., 2017) and can be shared across multiple tasks with the addition of a context signal (Cheung et al., 2019). By allowing the readout to adapt to new tasks, or by including context-signals, enabling the network to distinguish between different tasks and appropriately adjust its responses, the effective capacity that a learning algorithm can leverage could be higher, facilitating more plasticity and stability (Thorat et al., 2019; Hummos, 2022). However, it is not immediately clear how the RDAC framework could be extended to these scenarios, but accommodating them is essential for building a more versatile and adaptable framework for studying continual learning.

In closing, the RDAC framework not only provides a diagnostic tool to shed light on the intricate dynamics of stability and plasticity but also provides practical insights for the development of more robust continual learning algorithms. The journey of continual learning research continues, with our work offering a valuable contribution towards achieving the delicate balance between preserving past knowledge and adapting to new challenges in an ever-evolving world of information.

REPRODUCIBILITY STATEMENT

Details about the implementation of the continual learning algorithms are mentioned both in the Sections 4 and 5, and in the Appendix A.1. The gradient decomposition algorithm is derived and fully explained in Section 3.2.

ACKNOWLEDGMENTS

The project was funded by the European Union (ERC, TIME, Project 101039524), and by the research training group “Computational Cognition” (GRK2340) who are funded by the Deutsche Forschungsgemeinschaft (DFG; German Research Foundation). Compute resources were funded by the DFG (Project number 456666331).

REFERENCES

- Kyle Aitken, Marina Garrett, Shawn Olsen, and Stefan Mihalas. The geometry of representational drift in natural and artificial neural networks. *PLOS Computational Biology*, 18(11):e1010716, 2022.
- Daniel Anthes, Sushrut Thorat, Peter König, and Tim C Kietzmann. Diagnosing catastrophe: Large parts of accuracy loss in continual learning can be accounted for by readout misalignment. In *Conference on Cognitive Computational Neuroscience*, pp. 748–751, 2023.
- David L Barack and John W Krakauer. Two views on the cognitive brain. *Nature Reviews Neuroscience*, 22(6):359–371, 2021.
- Gail A Carpenter and Stephen Grossberg. A massively parallel architecture for a self-organizing neural pattern recognition machine. *Computer vision, graphics, and image processing*, 37(1): 54–115, 1987.
- Antonio Carta, Lorenzo Pellegrini, Andrea Cossu, Hamed Hemati, and Vincenzo Lomonaco. Avalanche: A pytorch library for deep continual learning. *arXiv preprint arXiv:2302.01766*, 2023.
- Brian Cheung, Alexander Terekhov, Yubei Chen, Pulkit Agrawal, and Bruno Olshausen. Superposition of many models into one. *Advances in neural information processing systems*, 32, 2019.
- MohammadReza Davari and Eugene Belilovsky. Probing representation forgetting in continual learning. In *NeurIPS 2021 Workshop on Distribution Shifts: Connecting Methods and Applications*, 2021.
- Matthias De Lange, Rahaf Aljundi, Marc Masana, Sarah Parisot, Xu Jia, Aleš Leonardis, Gregory Slabaugh, and Tinne Tuytelaars. A continual learning survey: Defying forgetting in classification tasks. *IEEE transactions on pattern analysis and machine intelligence*, 44(7):3366–3385, 2021.
- Laura N Driscoll, Noah L Pettit, Matthias Minderer, Selmaan N Chettih, and Christopher D Harvey. Dynamic reorganization of neuronal activity patterns in parietal cortex. *Cell*, 170(5):986–999, 2017.
- Laura N Driscoll, Lea Duncker, and Christopher D Harvey. Representational drift: Emerging theories for continual learning and experimental future directions. *Current Opinion in Neurobiology*, 76:102609, 2022.
- Robert M French. Catastrophic forgetting in connectionist networks. *Trends in cognitive sciences*, 3(4):128–135, 1999.
- Kaiming He, Xiangyu Zhang, Shaoqing Ren, and Jian Sun. Delving deep into rectifiers: Surpassing human-level performance on imagenet classification. In *Proceedings of the IEEE international conference on computer vision*, pp. 1026–1034, 2015.
- Ha Hong, Daniel LK Yamins, Najib J Majaj, and James J DiCarlo. Explicit information for category-orthogonal object properties increases along the ventral stream. *Nature neuroscience*, 19(4):613–622, 2016.
- Ali Hummos. Thalamus: a brain-inspired algorithm for biologically-plausible continual learning and disentangled representations. *arXiv preprint arXiv:2205.11713*, 2022.
- Tobias Kalb and Jürgen Beyerer. Causes of catastrophic forgetting in class-incremental semantic segmentation. In *Proceedings of the Asian Conference on Computer Vision*, pp. 56–73, 2022.
- Dongwan Kim and Bohyung Han. On the stability-plasticity dilemma of class-incremental learning. In *Proceedings of the IEEE/CVF Conference on Computer Vision and Pattern Recognition*, pp. 20196–20204, 2023.
- James Kirkpatrick, Razvan Pascanu, Neil Rabinowitz, Joel Veness, Guillaume Desjardins, Andrei A Rusu, Kieran Milan, John Quan, Tiago Ramalho, Agnieszka Grabska-Barwinska, et al. Overcoming catastrophic forgetting in neural networks. *Proceedings of the national academy of sciences*, 114(13):3521–3526, 2017.

-
- Yajing Kong, Liu Liu, Zhen Wang, and Dacheng Tao. Balancing stability and plasticity through advanced null space in continual learning. In *European Conference on Computer Vision*, pp. 219–236. Springer, 2022.
- Alex Krizhevsky, Geoffrey Hinton, et al. Learning multiple layers of features from tiny images. 2009.
- Yann LeCun, Léon Bottou, Yoshua Bengio, and Patrick Haffner. Gradient-based learning applied to document recognition. *Proceedings of the IEEE*, 86(11):2278–2324, 1998.
- Zhizhong Li and Derek Hoiem. Learning without forgetting. *IEEE transactions on pattern analysis and machine intelligence*, 40(12):2935–2947, 2017.
- David Lopez-Paz and Marc’Aurelio Ranzato. Gradient episodic memory for continual learning. *Advances in neural information processing systems*, 30, 2017.
- Paul Masset, Shanshan Qin, and Jacob A Zavatore-Veth. Drifting neuronal representations: Bug or feature? *Biological cybernetics*, 116(3):253–266, 2022.
- Michael McCloskey and Neal J Cohen. Catastrophic interference in connectionist networks: The sequential learning problem. In *Psychology of learning and motivation*, volume 24, pp. 109–165. Elsevier, 1989.
- Martial Mermillod, Aurélia Bugaïska, and Patrick Bonin. The stability-plasticity dilemma: Investigating the continuum from catastrophic forgetting to age-limited learning effects, 2013.
- Charles Micou and Timothy O’Leary. Representational drift as a window into neural and behavioural plasticity. *Current Opinion in Neurobiology*, 81:102746, 2023.
- Ari S Morcos, David GT Barrett, Neil C Rabinowitz, and Matthew Botvinick. On the importance of single directions for generalization. *arXiv preprint arXiv:1803.06959*, 2018.
- Martin Mundt, Yongwon Hong, Iuliia Pliushch, and Visvanathan Ramesh. A wholistic view of continual learning with deep neural networks: Forgotten lessons and the bridge to active and open world learning. *Neural Networks*, 160:306–336, 2023.
- German I Parisi, Ronald Kemker, Jose L Part, Christopher Kanan, and Stefan Wermter. Continual lifelong learning with neural networks: A review. *Neural networks*, 113:54–71, 2019.
- Vinay V Ramasesh, Ethan Dyer, and Maithra Raghu. Anatomy of catastrophic forgetting: Hidden representations and task semantics. *arXiv preprint arXiv:2007.07400*, 2020.
- Sylvestre-Alvise Rebuffi, Alexander Kolesnikov, Georg Sperl, and Christoph H Lampert. icarl: Incremental classifier and representation learning. In *Proceedings of the IEEE conference on Computer Vision and Pattern Recognition*, pp. 2001–2010, 2017.
- Sushrut Thorat, Giacomo Aldegheri, Marcel AJ Van Gerven, and Marius V Peelen. Modulation of early visual processing alleviates capacity limits in solving multiple tasks. *arXiv preprint arXiv:1907.12309*, 2019.
- Sushrut Thorat, Giacomo Aldegheri, and Tim C Kietzmann. Category-orthogonal object features guide information processing in recurrent neural networks trained for object categorization. In *SVRHM 2021 Workshop @ NeurIPS*, 2021.
- Gido M van de Ven, Tinne Tuytelaars, and Andreas S Tolias. Three types of incremental learning. *Nature Machine Intelligence*, 4(12):1185–1197, 2022.
- Liyuan Wang, Xingxing Zhang, Hang Su, and Jun Zhu. A comprehensive survey of continual learning: Theory, method and application. *arXiv preprint arXiv:2302.00487*, 2023.
- Shipeng Wang, Xiaorong Li, Jian Sun, and Zongben Xu. Training networks in null space of feature covariance for continual learning. In *Proceedings of the IEEE/CVF conference on Computer Vision and Pattern Recognition*, pp. 184–193, 2021.

Zeyuan Yang, Zonghan Yang, Yichen Liu, Peng Li, and Yang Liu. Restricted orthogonal gradient projection for continual learning. *AI Open*, 2023.

Friedemann Zenke, Ben Poole, and Surya Ganguli. Continual learning through synaptic intelligence. In *International conference on machine learning*, pp. 3987–3995. PMLR, 2017.

Zhen Zhao, Zhizhong Zhang, Xin Tan, Jun Liu, Yanyun Qu, Yuan Xie, and Lizhuang Ma. Rethinking gradient projection continual learning: Stability/plasticity feature space decoupling. In *Proceedings of the IEEE/CVF Conference on Computer Vision and Pattern Recognition*, pp. 3718–3727, 2023.

A APPENDIX

A.1 METHODS

A.1.1 DEEP NON-LINEAR NETWORK EXPERIMENTS

For the experiments on the Cifar10 task we construct 11 datasets (one for each task). The first task, on which we perform the bulk of our analyses consists of the full Cifar10 dataset (with usual training and validation splits). For each subsequent task, we sample 10 unique classes from Cifar100. Experiments are repeated with three different repeats of this procedure, providing some control for varying difficulty of the different task splits. Data for all tasks was augmented with random cropping (padding = 4) and horizontal flipping throughout training. All data was normalized with means (0.5071, 0.4865, 0.4409) and standard deviations (0.2673, 0.2564, 0.2762) for the RGB channels.

All networks were trained with Adam ($lr = 0.001$, $\beta_1 = 0.9$, $\beta_2 = 0.999$) for 60 epochs per task. Following the findings in Li & Hoiem (2017), we warm up the new readout at the start of each new task (excluding training on the first task). This has been reported to stabilize representations at the start of training on a new task (where the randomly initialized new readout is not aligned with the features of the remainder of the network, causing large gradients). We freeze the weights of all layers except the new readout for the first 10 epochs of training. Additionally, since our analyses investigate activation changes relative to the range of previously learned readouts, we freeze all parameters in old readouts for methods that would otherwise allow changing readout weights for old tasks (this is the case for LwF and data replay).

The network architecture for these experiments is adopted from Zenke et al. (2017) and has been slightly altered. It consists of two VGG blocks (32 channels in the first, 64 channels in the second block each, kernel size 3). Each block of two convolutional layers is followed by a max pool layer with kernel size and stride 2. The pre-readout dense layer was scaled to have 128 output units and no dropout was used throughout the network. All layers in the backbone were initialized with Kaiming-He He et al. (2015) initialisation as implemented in PyTorch.

After performing initial sweeps for the hyperparameters in the tested algorithms to determine the rough effective ranges, we performed additional sweeps for each algorithm in order to generate the datapoints in figure 2. Each datapoint visualised is the average over three experiments with the same hyperparameter settings, but different seeds (and therefore task splits as described above).

Hyperparameters were swept as follows:

- For EWC, λ was varied between $1e - 1$ - $1e5$.
- For SI, ϵ was fixed to 1 and λ was varied between $1e - 2$ and $1e5$.
- For LwF, we fixed the temperature to 1 and varied alpha between 0.01 and 10.
- For data replay, we used replay buffer sizes between 0 and 60000 samples, with the default replay buffer style as implemented in Avalanche (as of version 0.3.1).
- For GEM, we varied the memory strength parameter (γ in the original publication) between 0 and 1 and varied the number of patterns stored per experience to estimate the gradient projection between 0 and 20000.

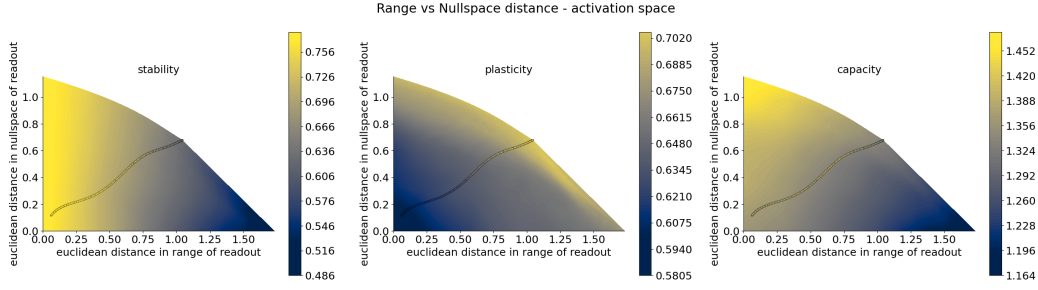


Figure 4: Movement in range and null space for gradient decomposition (surface) and EWC (scatter points). Points and contours are coloured by plasticity, stability and "capacity" computed as plasticity + stability.

A.1.2 ONE-HIDDEN LAYER LINEAR NETWORK EXPERIMENTS

The linear system described in section 5 is a one hidden layer network without biases and 11 units in its hidden layer. The network has two separate linear readouts with 5 units each, to accommodate the split MNIST task. For all experiments, the network was trained for 30 epochs per task, with plain stochastic gradient descent and a learning rate $5 \cdot 10^{-4}$ and batch size 16. Since the Split MNIST task is very easy, even for a small linear network we increase the difficulty of the dataset slightly by applying a number of transformations to the dataset once at the time of constructing the dataset. This increases the effect of catastrophic forgetting while keeping a fixed dataset, allowing for easy experimentation. The transformations were implemented using the torchvision transforms package. Images of digits were augmented with random rotations (± 10 degrees), translations (± 10 percent of image size in both axes), scaled between 90-110% of the original size and randomly cropped with padding = 4. Finally, we applied the 'ColorJitter' transformation with parameters brightness = 0.1, contrast = 0.1, saturation = 0.1 and hue = 0.1. Transformations are only applied to training data for both tasks.

For EWC, we approximate the diagonal of the Fisher information matrix for the hidden layer parameters as the square of the gradients for the first task over the whole dataset for task 1.

$$F_w = \frac{\sum_N (\Delta w)^2}{N}$$

For N batches of data. We sweep 1000 values for the scalar multiplier λ governing regularization strength on a log scale between 0 and 10^5 .

To illustrate our gradient decomposition result, we swept the space of possible decompositions in a grid with 33 linear spaced values between 0 and 1 for α and β . In Figure 3 we visualized the extremes of this search, and the results of the full space are included in Figure 4 for completeness.